Effects of Parathyroid Hormone and Calcitonin on Bone Formation and Resorption: Mathematical Modeling Approach

Inthira Chaiya, Chontita Rattanakul, Sahattaya Rattanamongkonkul, Wannapa Kunpasuruang,

and Sittipong Ruktamatakul

***Abstract*—**A system of nonlinear differential equations is proposed here to describe the mechanism of bone formation and resorption based on the effects of parathyroid hormone and calcitonin. Singular perturbation technique is then applied to the model in order to obtain the conditions on the system parameters for which the various kinds of dynamics behavior can be occurred. Computer Simulations are also carried out to support our theoretical predictions. Both of theoretical result and numerical result show that a periodic solution of the model can be expected for a certain set of parametric values corresponding to the pulsatile secretions of parathyroid hormone and calcitonin reported in clinical evidences.

***Keywords*—**bone formation, bone resorption, calcitonin, mathematical model, parathyroid hormone.

I. Introduction

OSTEOPOROSIS is a major bone disease characterized by low bone mass, the structural deterioration of bone and an increased risk of fracture [1], [2]. It is a bone disease where bone mass decreases over time resulting from the net increase of bone resorption over bone formation after each remodeling cycle occur [1]-[3]. Bone remodeling is a process that occurs by the team work of two types of cells which are osteoclastic cells and osteoblastic cells. The process starts with the activation of the remodeling site followed by the resorption of bone by osteoclastic cells and the formation of bone by osteoblastic cells [4]-[6]. There are several factors involve in the process such as parathyroid hormone (PTH), calcitonin (CT), vitamin D and estrogen. Therefore, the knowledge of the differentiation and proliferation of osteoblasts and osteoclasts including the regulation of hormones which have impact on the process of differentiation and proliferation of osteoblasts and osteoclasts is needed.

Even though there are many attempts to develop a mathematical model to describe the mechanism of bone formation and resorption [7]-[10], none of them incorporate the effects of both of PTH and CT. Therefore, we will develop a mathematical model to describe bone remodeling process based on the effects of PTH and CT by modifying the model that has been proposed by Rattanakul *et al.* [8].

Manuscript received August 1, 2011. This work was supported by the Centre of Excellence in Mathematics, Commission on Higher Education, Thailand.

I. Chaiya is with the Department of Mathematics, Faculty of Sciences, Mahidol University, Thailand and the Centre of Excellence in Mathematics, the Commission on Higher Education, Thailand (e-mail: g5237102@student.mahidol.ac.th).

C. Rattanakul is with the Department of Mathematics, Faculty of Sciences, Mahidol University, Thailand and the Centre of Excellence in Mathematics, the Commission on Higher Education, Thailand (corresponding author, phone: 662-201-5340; fax: 662-201-5343; e-mail: sccrt@mahidol.ac.th).

S. Rattanamongkonkul is with the Department of Mathematics, Faculty of Sciences, Burapha University, Thailand and the Centre of Excellence in Mathematics, the Commission on Higher Education, Thailand (e-mail: sahattay@buu.ac.th).

W. Kunpasuruang is with the Department of Mathematics, Faculty of Science, Silpakorn University, Thailand and the Centre of Excellence in Mathematics, the Commission on Higher Education, Thailand (e-mail: wannapa@su.ac.th).

S. Ruktamatakul is with the Department of Mathematics, Faculty of Liberal Arts Science, Kasetsart University, Thailand and the Centre of Excellence in Mathematics, the Commission on Higher Education, Thailand (e-mail: faasspr@nontri.ku.ac.th).

II. Model Modification

Let us denote the concentration of PTH above the basal level in blood at time t by $X(t)$, the concentration of CT above the basal level in blood at time t by $Y(t)$, the number of active osteoclasts at time t by $Z(t)$, and the number of active osteoblasts at time t by $W(t)$. Assuming that the high levels of osteoclast and osteoblast precursors lead to the high levels of active osteoclastic and osteoblastic cells, respectively, which result from the differentiation, and activation of their precursors, we then propose a mathematical model of bone formation and resorption as follows.

PTH is secreted from the parathyroid gland. It is directly controlled by the level of calcium in blood. The decrease of calcium level in blood results in an increase in the secretion of PTH from the parathyroid grand [11]. On the other hand, osteoclasts resorb bone and release calcium and hence the more osteoclasts mean the more elevation in the serum level of calcium. Therefore, there is an inverse relationship between the number of active osteoclasts and the secretion of PTH [11]. The equation for the rate of PTH secretion above the basal level is then assumed to take the form

$$\frac{dX}{dt} = \frac{a_1}{k_1 + Z} - b_1 X \tag{1}$$

where the first term on the right-hand side of (1) represents the secretion rate of PTH from the parathyroid gland, while a_1 and k_1 are positive constants. The last term on the right-hand side is the removal rate of PTH from the system with the removal rate constant b_1.

CT is produced by the thyroid gland [12]. In opposite to PTH, the secretion of CT is stimulated by elevated serum calcium level. CT inhibits osteoclastic activity in bone resorption leading to the decrease in the serum level of calcium [12]. Therefore, the equation for the rate of calcitonin secretion is then assumed to have the form

$$\frac{dY}{dt} = \left(a_2 - a_3 Y\right) YZ - b_2 Y \tag{2}$$

where the first term on the right-hand side of (2) represents the secretion rate of CT from the thyroid gland. The last term is the removal rate constant b_2. a_2 and a_3 are positive constants.

Osteoclast is bone resorbing cell. It originates from from hemopoietic stem cells of the monocyte/macrophage lineage [1]. There are several factors that regulate osteoclast formation and differentiation such as osteoclast differentiation factor (ODF) which was found to be identical to osteoprotegerin ligand (OPGL), TNF-related activation induces cytokine (TRANCE), receptor activator NF-kB ligand (RANKL) [7], [13]-[15]. Moreover, osteoblast is necessary for the differentiation and activation of osteoclast since it possesses RANKL which requires for the differentiation of osteoclast [7], [13]. On the other hand, PTH also stimulates the differentiation of osteoclast indirectly which requires the presence of osteoblasts since osteoclasts and their precursors do not possess PTH receptors while osteoblasts and their precursors possess them [7], [13], [16]. However, it has been reported that when the level of PTH increases further, the production of osteoclasts will be decreased [7]. Therefore, the dynamics of the active osteoclastic population can be described by the following equation

$$\frac{dZ}{dt} = \left(\frac{a_4 + a_5 X}{k_2 + X^2} - a_6 Y\right) ZW - b_3 Z \tag{3}$$

where the first term on the right-hand side of (3) represents the stimulating effect of PTH and the inhibiting effect of CT on active osteoclasts reproduction [17]-[19]. The last term on the right-hand side is the removal rate of active osteoclasts from the system with the removal rate constant b_3. a_4, a_5, a_6 and k_2 are positive constants.

Osteoblast is bone forming cell. It is derived from the mesenchymal stem cells. There are many factors involve in the proliferation and differentiation of osteoblasts such as FGF, IGF-I, TGF-beta, including PTH [1], [7]. Moreover, PTH stimulates the differentiation of osteoblasts and extends their working life by preventing their death through a suicidal process called apoptosis [21], [22]. However, it has also been reported that PTH exerts both stimulating and inhibiting effects on the osteoblastic differentiation process depending on the differentiation stages [1]. The dynamics of the osteoblastic population can be described by the following equation

$$\frac{dW}{dt} = \frac{a_7 X}{k_3 + X} - \frac{a_8 XW}{k_4 + X} - b_4 W \tag{4}$$

where the first term on the right-hand side of (4) represents the reproduction of active osteoblasts through the stimulating effect of PTH on osteoblastic cells, while the second term on the right-hand side of (4) represents the inhibiting effect of PTH on osteoblastic differentiation [23]. The last term is the removal rate of osteoblasts from the system. a_7, a_8, k_3, k_4 and b_4 are positive constants.

III. SINGULAR PERTURBATION ANALYSIS

In order to apply the singular perturbation technique to our model, we then assume that PTH has the fastest dynamics, CT has the fast dynamics. The osteoclastic population has the slow dynamics and the osteoblastic population has the slowest dynamics. Consequently, we scale the dynamics of the four components and parameters of the system in term of small positive parameters $0 < \varepsilon << 1$, $0 < \delta << 1$ and $0 < \eta << 1$ as follows.

Letting $x = X, y = Y, z = Z, w = W, c_1 = a_1, c_2 = \frac{a_2}{\varepsilon}, c_3 = \frac{a_3}{\varepsilon}$, $c_4 = \frac{a_4}{\varepsilon\delta}, c_5 = \frac{a_5}{\varepsilon\delta}, c_6 = \frac{a_6}{\varepsilon\delta}, c_7 = \frac{a_7}{\varepsilon\delta\eta}, c_8 = \frac{a_8}{\varepsilon\delta\eta}, d_1 = b_1, d_2 = \frac{b_2}{\varepsilon}$, $d_3 = \frac{b_3}{\varepsilon\delta}, d_4 = \frac{b_4}{\varepsilon\delta\eta}$, we are led to the following model equations:

$$\frac{dx}{dt} = \frac{c_1}{k_1 + z} - d_1 x \equiv f\left(x, y, z, w\right) \tag{5}$$

$$\frac{dy}{dt} = \varepsilon\left(\left(c_2 - c_3 y\right) yz - d_2 y\right) \equiv \varepsilon g\left(x, y, z, w\right) \tag{6}$$

$$\frac{dz}{dt} = \varepsilon\delta\left(\left(\frac{c_4 + c_5 x}{k_2 + x^2} - a_6 y\right) zw - d_3 z\right) \equiv \varepsilon\delta h\left(x, y, z, w\right) \tag{7}$$

$$\frac{dw}{dt} = \varepsilon\delta\eta\left(\frac{c_7 x}{k_3 + x} - \frac{c_8 xw}{k_4 + x} - d_4 w\right) \equiv \varepsilon\delta\eta k\left(x, y, z, w\right) \tag{8}$$

The system of (5)-(8), with the small parameters ε, δ and η can then be analyzed by using the geometric singular perturbation method.

The manifold $\{f = 0\}$

This manifold is given by the equation

$$x = \frac{c_1}{d_1\left(k_1 + z\right)} \equiv A\left(z\right) \tag{9}$$

We see that this manifold is independent of y and w. Hence, it is parallel to the *y*-axis and *w*-axis. It intersects the *x*-axis at the point where

$$x = \frac{c_1}{d_1 k_1} \equiv x_1 \tag{10}$$

Moreover, $A(z)$ is an decreasing function of z and $A(z) \to 0$ as $z \to \infty$.

The manifold $\{g = 0\}$

This manifold consists of two submanifolds. One is the trivial manifold $y = 0$. The nontrivial one given by the equation

$$y = \frac{c_2 z - d_2}{c_3 z} \equiv B(z) \tag{11}$$

This nontrivial manifold is independent of the variable *x* and *w*. Hence, this submanifold is parallel to the x-axis and *w*-axis. It intersects the *z*-axis at the point where

$$z = \frac{d_2}{c_2} \equiv z_1 \tag{12}$$

Moreover, $B(z)$ is an increasing function of *z* and $B(z)$ is asymptotic to the line

$$y = \frac{c_2}{c_3} \equiv y_1 \tag{13}$$

as $z \to \infty$.

On the other hand, the manifold $\{f = 0\}$ intersects the manifold $\{g = 0\}$ along the curve

$$\left\{ x = \frac{c_1}{d_1 (k_1 + z)}, y = 0 \right\}$$

and the curve

$$\left\{ x = \frac{c_1}{d_1 (k_1 + z)}, y = \frac{c_2 z - d_2}{c_3 z} \right\}$$

The manifold $\{h = 0\}$

This manifold consists of two sub-manifolds. One is the trivial manifold $z = 0$ while the other one is the nontrivial manifold

$$y = \frac{1}{c_6}\left(\frac{c_4 + c_5 x}{k_2 + x^2} - \frac{d_3}{w} \right) \equiv C(x,w) \tag{14}$$

which is independent of *z* and hence, it is parallel to the *z*-axis. $C(x,w)$ attains its maximum at the points where

$$x = \frac{-c_4 + \sqrt{c_4^{\,2} + c_5^{\,2} k_2}}{c_5} \equiv x_M \tag{15}$$

and

$$y(w) = \frac{1}{c_6}\left(\frac{c_4 + c_5 x_2}{k_2 + x_2^2} - \frac{d_3}{w} \right) \equiv y_M(w) \tag{16}$$

Note that $y_M(w) > 0$ if and only if

$$w > \frac{d_3 (k_2 + x_2^2)}{c_4 + c_5 x_2} \tag{18}$$

For a fixed value of *w*, the nontrivial manifold $y = C(x,w)$ intersects the *y*-axis at the point where $x = 0$ and

$$y = \frac{1}{c_6}\left(\frac{c_4}{k_2} - \frac{d_3}{w} \right) \equiv y_2(w) \tag{17}$$

Note that $y_2(w) > 0$ if and only if

$$w > \frac{d_3 k_2}{c_4} \tag{18}$$

On the other hand, for a fixed value of *w*, the nontrivial manifold $y = C(x,w)$ intersects the *x*-axis at the point where $y = 0$ and

$$x = \frac{c_5 w + \sqrt{(c_5 w)^2 + 4 d_3 (c_4 w - d_3 k_2)}}{2 d_3} \equiv x_2(w) \tag{19}$$

Note that if $y_2(w) > 0$ then $x_2(w) > 0$.

Moreover, $y = C(x,w)$ is an increasing function of *w* and for a fixed value of x, $y \to \frac{1}{c_6}\left(\frac{c_4 + c_5 x}{k_2 + x^2} \right)$ as $w \to \infty$.

In addition, the manifold $\{f = 0\}$ intersects the manifold $\{h = 0\}$ along the line

$$\{x = x_1, z = 0\}$$

and the curve

$$\left\{ x = \frac{c_1}{d_1 (k_1 + z)}, y = \frac{1}{c_6}\left[\left(\frac{c_4 + c_5 x}{k_2 + x^2} \right) - \frac{d_3}{w} \right] \right\}$$

which attains its relative maximum at the points where

$$x = x_M, y = y_M, \text{ and } z = \frac{1}{d_1}\left(\frac{c_1}{x_M} - d_1 k_1 \right) \equiv z_M$$

Note that $z_M > 0$ if and only if $x_M < \frac{c_1}{d_1 k_1}$.

Moreover, the manifold $\{f = 0\}$ intersects the manifold $\{g = 0\}$ and the manifold $\{h = 0\}$ at the point where

$$\{x = x_1, y = 0, z = 0\},$$

$$\{x = x_{S_1}(w), y = 0, z = z_{S_1}(w)\},$$

and $$\{x = x_{S_2}(w), y = y_{S_2}(w), z = z_{S_2}(w)\}$$

where $x_{S_1}(w) = \frac{c_5 w \pm \sqrt{(c_5 w)^2 + 4 d_3 (c_4 w - d_3 k_2)}}{2 d_3}$,

$$z_{S_1}(w) = \frac{1}{d_1}\left(\frac{c_1}{x_{S_1}} - d_1 k_1 \right).$$

$y_{S_2}(w)$ is a positive solution of

$$A_1(w) y^3 + A_2(w) y^2 + A_3(w) y + A_4(w) = 0$$

where

$$A_1(w) = c_3^2 c_6 w\left(d_1^2 k_1^2 k_2 + c_1^2\right)$$
$$A_2(w) = -2c_3 c_6 d_1^2 k_1 k_2 w\left(d_2 + c_2 k_1\right) - c_3^2 d_1^2 k_1^2\left(c_4 w - d_3 k_2\right) - c_1 c_3\left(2c_1 c_2 c_6 w + c_3 c_5 d_1 k_1 w - c_1 c_3 d_3\right)$$
$$A_3(w) = c_1^2 c_2\left(-2c_3 d_3 + c_2 c_6 w\right) + c_1 c_3 c_5 d_1 w\left(d_2 + 2c_2 k_1\right) + c_6 d_1^2 k_2 w\left(d_2 + c_2 k_1\right)^2 + 2c_3 d_1^2 d_2 k_1\left(c_4 w - d_3 k_2\right) + 2c_2 c_3 d_1^2 k_1^2\left(c_4 w - d_3 k_2\right)$$
$$A_4(w) = -c_1 c_2 c_5 d_1 w\left(d_2 + c_2 k_1\right) - d_1^2\left(d_2 + c_2 k_1\right)^2\left(c_4 w - d_3 k_2\right) + c_1^2 c_2^2 d_3$$

and $z_{S_2}(w) = \dfrac{d_2}{c_2 - c_3 y_{S_2}}$, $x_{S_2}(w) = \dfrac{c_1}{d_1\left(k_1 + z_{S_2}\right)}$.

The manifold { k = 0 }

This manifold is given by the equation

$$w = \frac{c_7 x^2 + c_7 k_4 x}{\left(c_8 + d_4\right)x^2 + \left(c_8 k_3 + d_4 k_3 + d_4 k_4\right)x + d_4 k_3 k_4} \equiv \Psi(x) \quad (20)$$

This manifold is independent of y and z. It intersects the x-axis at the point where $w = 0$ and $x = 0$ or $x = -k_4$, while it intersects the w-axis at the point where $x = 0$ and $w = 0$. Moreover, $w \to \dfrac{c_7}{c_8 + d_4}$ as $x \to \infty$. On the other hand, $w \to \infty$ as $x \to x_4$ where

$$x_3 \equiv \frac{-\left(c_8 k_3 + d_4 k_3 + d_4 k_4\right)}{2\left(c_8 + d_4\right)} \pm \frac{\sqrt{\left(c_8 k_3 + d_4 k_3 + d_4 k_4\right)^2 - 4d_4 k_3 k_4\left(c_8 + d_4\right)}}{2\left(c_8 + d_4\right)} < 0 \quad (21)$$

We now identify and analyze each of the three possible cases as shown in Fig. 1 through Fig. 3 as follows.

Case I: If ε and δ are sufficiently small and the inequalities

$$0 < x_M < x_1 < x_2(w) \quad (22)$$
$$0 < z_{S_2}(w) < z_M \quad (23)$$
$$y_2(w) > 0 \quad (24)$$
$$x_{S_2}(w) > 0, y_{S_2}(w) > 0, z_{S_2}(w) > 0 \quad (25)$$

are satisfied where all parametric values are defined as above, then the manifolds are positioned as in Fig. 1 and the system of (5)-(8) will have a periodic solution. Here, the transitions of slow, fast and fastest speeds are indicated by one, two and three arrows, respectively.

In Fig. 1, without loss of generality we start from point *A* and we assume that the position of *A* is as in Fig. 1 with $\{f \neq 0\}$. A fastest transition will tend to point *B* on the manifold $\{f = 0\}$. Here, $\{g < 0\}$ and a transition at fast speed will be made in the direction of decreasing y until point *C* on the curve $\{f = h = 0\}$ is reached. A fast transition then follows along this curve to some point *D* on the other stable part of $\{f = h = 0\}$ followed by a fast transition in the direction of decreasing y until the point *E* is reached since $\{g < 0\}$ here. Once the point *E* is reached the stability of submanifold will be lost. A jump to point *F* on the other stable part of $\{f = h = 0\}$ followed by a fast transition in the direction of increasing y since $\{g > 0\}$ here. Once the point *G* is reached the stability of submanifold will be lost. A jump to point *H* on the other stable part of $\{f = h = 0\}$. Consequently, a fast transition will bring the system back to the point *E*, followed by flows along the same path repeatedly, resulting in the closed orbit *EFGHE*. Thus, limit cycle in the system for ε, δ and η are sufficiently small exists.

Case II: If ε and δ are sufficiently small and the inequalities

$$0 < x_M < x_1 < x_2(w) \quad (26)$$
$$0 < z_M < z_{S_2}(w) \quad (27)$$
$$y_2(w) > 0 \quad (28)$$
$$x_{S_2}(w) > 0, y_{S_2}(w) > 0, z_{S_2}(w) > 0 \quad (29)$$

are satisfied where all the parametric values are given as above, then the manifolds are positioned as in Fig. 2 and the system of (5)-(8) will have a stable equilibrium point.

In Fig. 2, without loss of generality we start from point *A* and we assume that the position of *A* is as in Fig. 2 with $\{f \neq 0\}$. A fastest transition will tend to point *B* on the manifold $\{f = 0\}$. Here, $\{g < 0\}$ and a transition at fast speed will be made in the direction of decreasing y until point *C* on the curve $\{f = h = 0\}$ is reached. A fast transition then follows along this curve to some point *D* on the other stable part of $\{f = h = 0\}$ followed by a fast transition in the direction of decreasing y until the point *E* is reached since $\{g < 0\}$ here. Once the point *E* is reached the stability of submanifold will be lost. A jump to point *F* on the other stable part of $\{f = h = 0\}$ followed by a fast transition in the direction of increasing y until the steady state S_2 where $f = g = h = 0$ is reached since $\{g > 0\}$ here. Thus, the solution trajectory is expected in this case to tend toward this stable equilibrium point S_2 as time passes.

Case III: If ε and δ are sufficiently small and the inequalities

$$0 < x_M < x_2(w) < x_1 \quad (30)$$
$$0 < z_M < z_{S_2}(w) \quad (31)$$
$$y_2(w) > 0 \quad (32)$$
$$x_{S_2}(w) > 0, y_{S_2}(w) > 0, z_{S_2}(w) > 0 \quad (33)$$

are satisfied where all the parametric values are given as above, then the manifolds are positioned as in Fig. 3 and the system of (5)-(8) will have a stable equilibrium point.

In Fig. 3, without loss of generality we start from point *A* and we assume that the position of *A* is as in Fig. 3 with $\{f \neq 0\}$. A fastest transition will tend to point *B* on the manifold $\{f = 0\}$. Here, $\{g < 0\}$ and a transition at fast speed will be made in the direction of decreasing y until point *C* on the curve $\{f = g = 0\}$ is reached. A slow transition then follows along this curve in the direction of increasing *z* until the steady state S_1 where $f = g = h = 0$ is reached since $\{h > 0\}$ here. Thus, the solution trajectory is expected in this case to tend toward this stable equilibrium point S_1 as time passes.

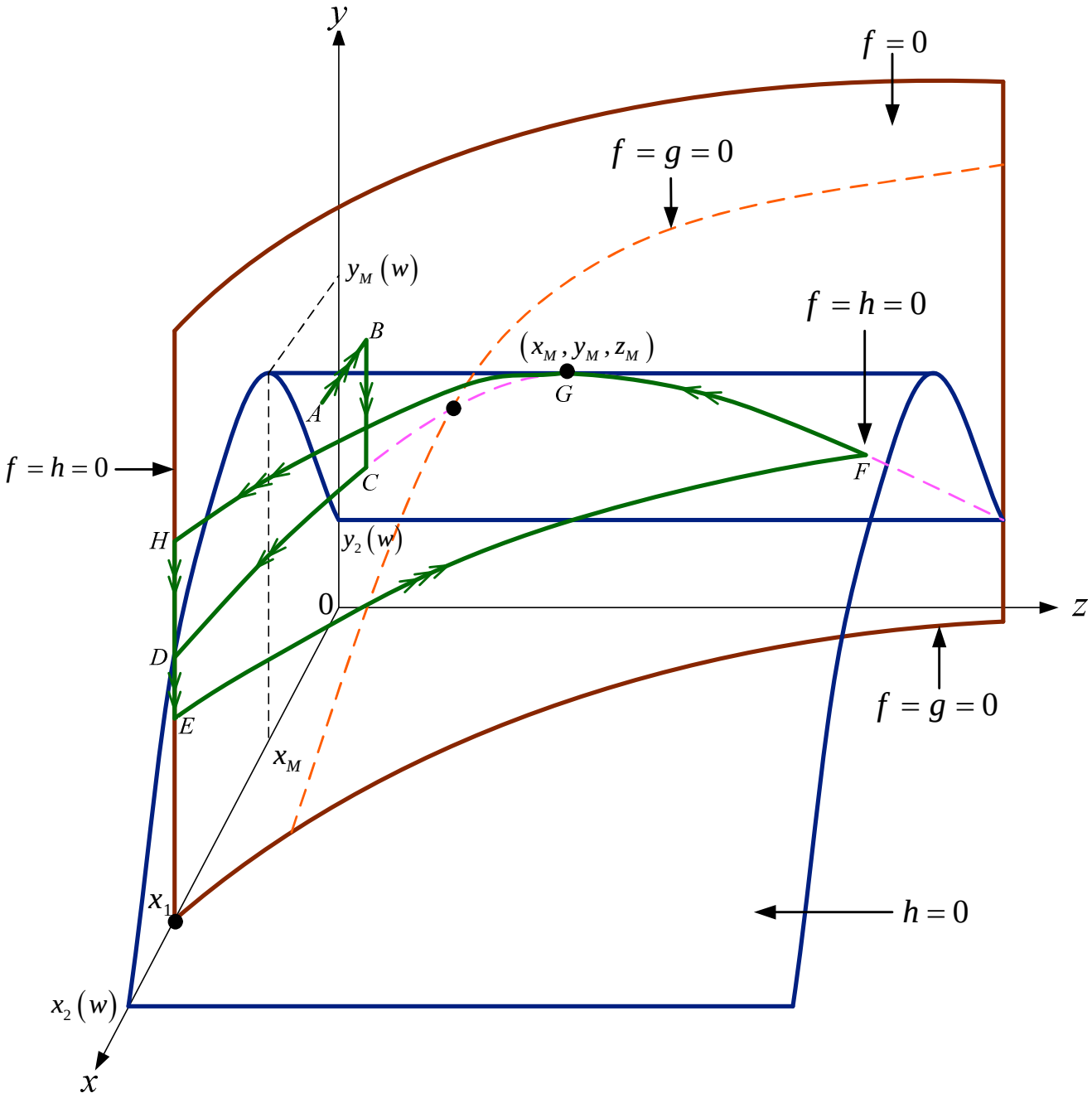

Fig. 1 The three equilibrium manifolds $\{f = 0\}, \{g = 0\}$ and $\{h = 0\}$ in the (x, y, z) – space in the case 1. Segments of the trajectories with one, two, and three arrows represent slow, fast, and fastest transitions, respectively.

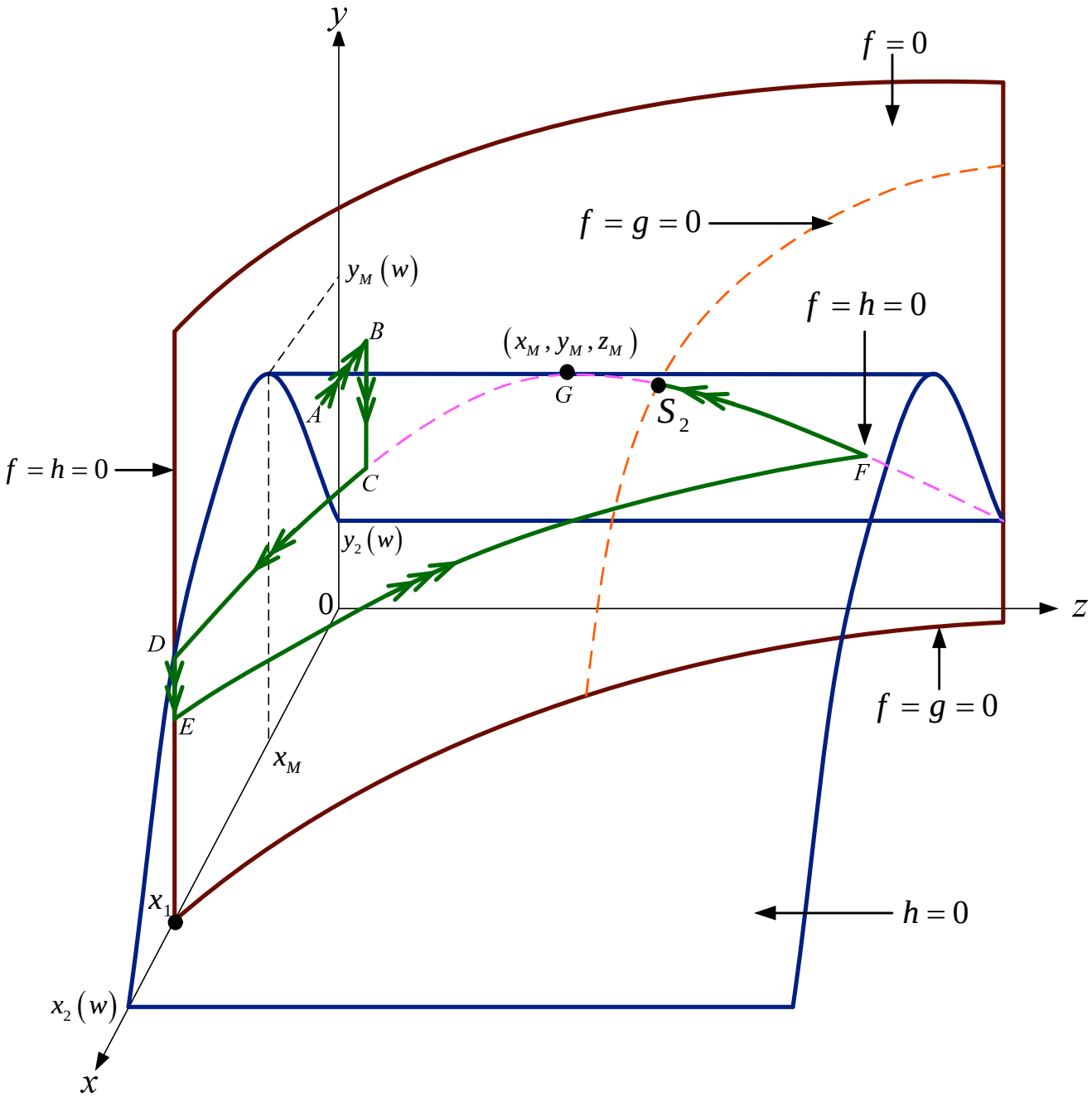

Fig. 2 The three equilibrium manifolds $\{f=0\},\{g=0\}$ and $\{h=0\}$ in the (x,y,z)– space in the case 2. Segments of the trajectories with one, two, and three arrows represent slow, intermediate, and fast transitions, respectively.

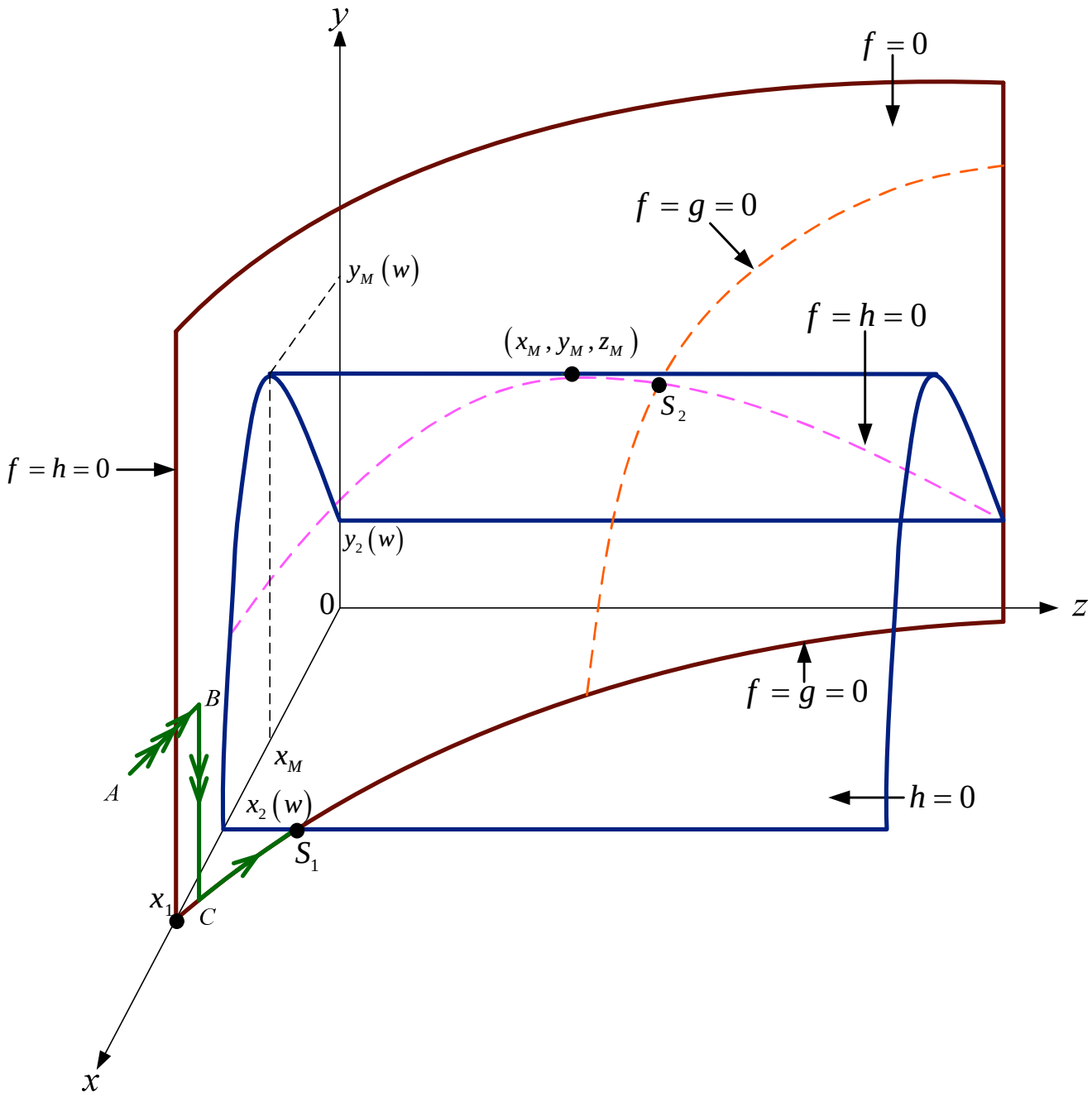

Fig. 3 The three equilibrium manifolds $\{f=0\},\{g=0\}$ and $\{h=0\}$ in the $(x,y,z)-$ space in the case 3. Segments of the trajectories with one, two, and three arrows represent slow, intermediate, and fast transitions, respectively.

IV. NUMERICAL RESULTS

A computer simulation of the system (5)-(8) is presented in Fig. 4, with parametric values chosen to satisfy the condition in Case 1. The solution trajectory, shown in Fig. 4(a) project onto the (x,y)-plane, tends to a limit cycle as theoretically predicted. The corresponding time courses of the concentration of parathyroid hormone and calcitonin above the basal levels are as shown in Fig. 4(b) and 4(c), respectively.

A computer simulation of the system (5)-(8) is presented in Fig. 5, with parametric values chosen to satisfy the condition in Case 2. The solution trajectory, shown in Fig. 5(a) project onto the (x,y)-plane, tends to a limit cycle as

theoretically predicted. The corresponding time courses of the concentration of parathyroid hormone and calcitonin above the basal levels are as shown in Fig. 5(b) and 5(c), respectively.

A computer simulation of the system (5)-(8) is presented in Fig. 6, with parametric values chosen to satisfy the condition in Case 3. The solution trajectory, shown in Fig. 6(a) project onto the (x, y)-plane, tends to a limit cycle as theoretically predicted. The corresponding time courses of the concentration of parathyroid hormone and calcitonin above the basal levels are as shown in Fig. 6(b) and 6(c), respectively.

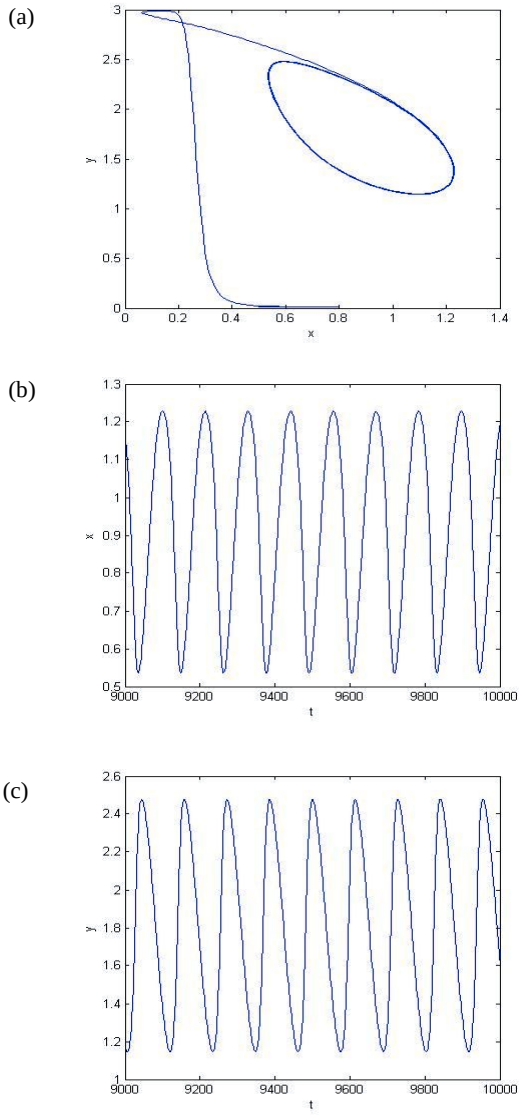

Fig. 4 A computer simulation of the model systems (5)-(8) with $\varepsilon = 0.9,\ \delta = 0.5,\ \eta = 0.3,\ c_1 = 0.3,\ c_2 = 0.3,\ c_3 = 0.1,\ c_4 = 0.4,$ $c_5 = 0.9, c_6 = 0.3, c_7 = 0.5, c_8 = 0.2, d_1 = 0.5, d_2 = 0.03, d_3 = 0.25,$ $d_4 = 0.2, k_1 = 0.4, k_2 = 0.6, k_3 = 0.5, k_4 = 0.03, x(0) = 0.5, y(0) = 0.01,$ $z(0)=0.05$ and $w(0)=3.5$. (a) The solution trajectory projected onto the (x,y)-plane. (b) The corresponding time courses of PTH (x), and (c) CT level (y).

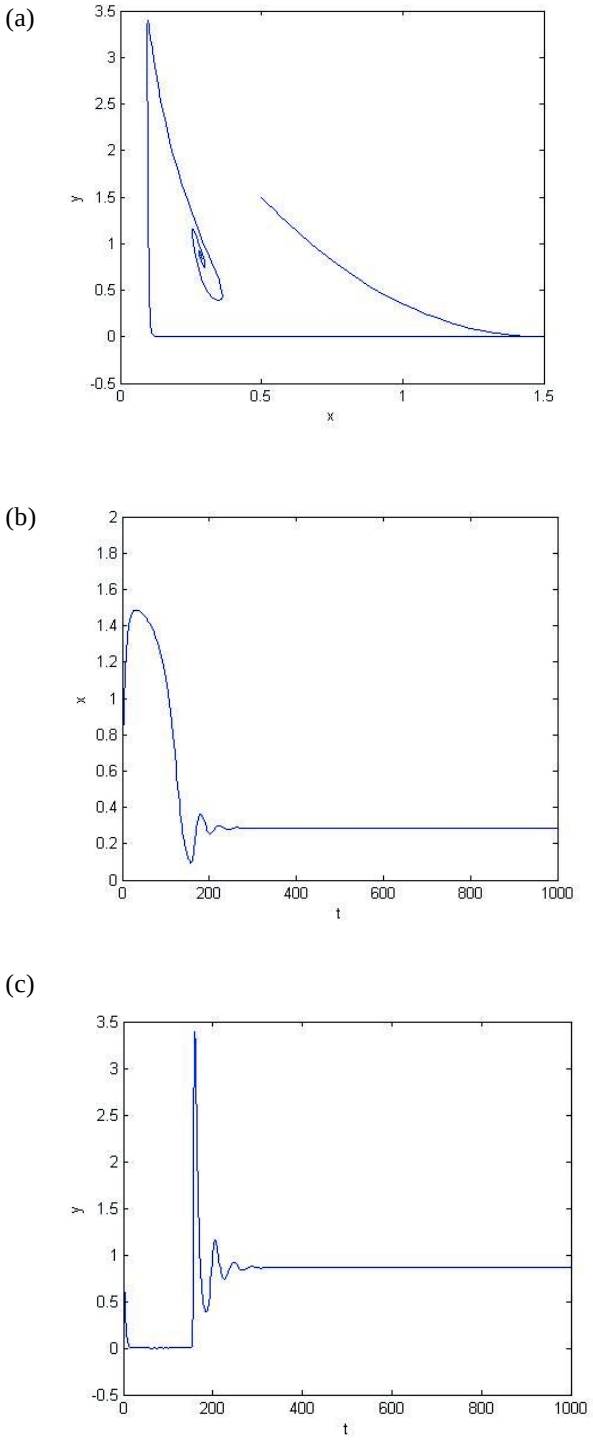

Fig. 5 A computer simulation of the model systems (5)-(8) with $\varepsilon = 0.4,\ \delta = 0.5,\ \eta = 0.3,\ c_1 = 0.1,\ c_2 = 0.5,\ c_3 = 0.1,\ c_4 = 0.2,$ $c_5 = 0.9, c_6 = 0.5, c_7 = 0.7, c_8 = 0.5, d_1 = 0.15, d_2 = 0.8, d_3 = 0.4,$ $d_4 = 0.3, k_1 = 0.4, k_2 = 0.4, k_3 = 0.1, k_4 = 0.1, x(0) = 0.5, y(0) = 1.5,$ $z(0)=0.05$ and $w(0)=0.5$. (a) The solution trajectory projected onto the (x,y)-plane. (b) The corresponding time courses of PTH (x), and (c) CT level (y).

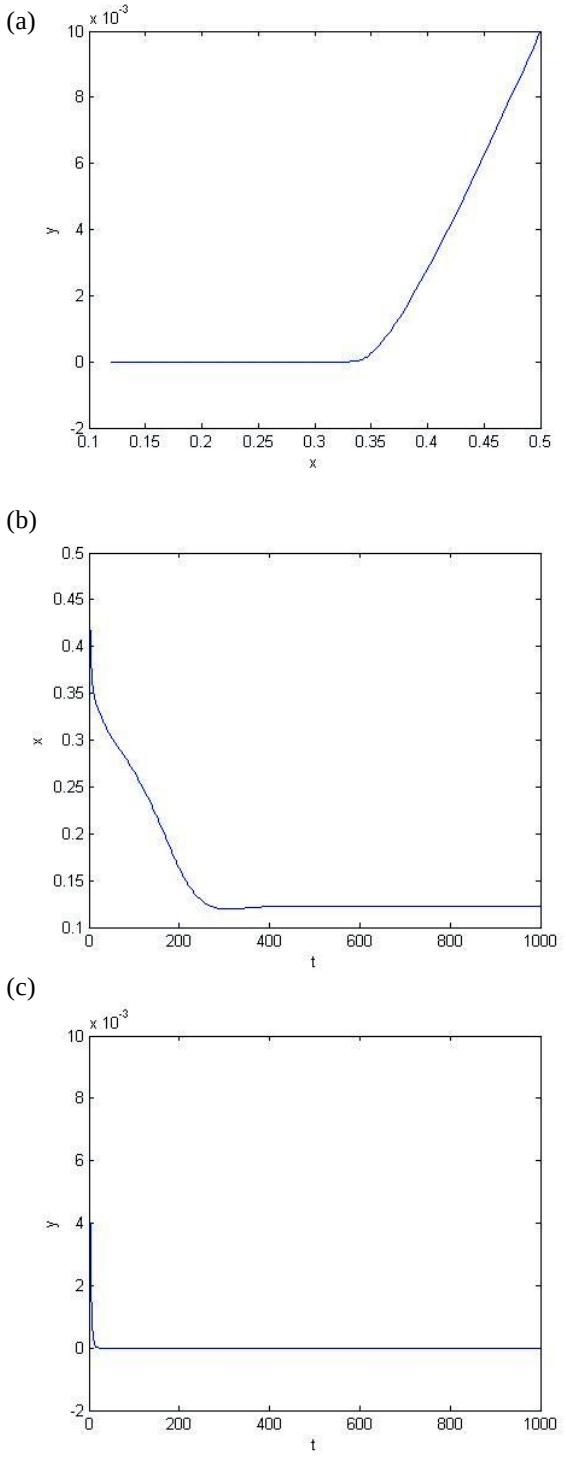

Fig. 6 A computer simulation of the model systems (5)-(8) with $\varepsilon = 0.7$, $\delta = 0.7$, $\eta = 0.3$, $c_1 = 0.1$, $c_2 = 0.05$, $c_3 = 0.1$, $c_4 = 0.1$, $c_5 = 0.03$, $c_6 = 0.2$, $c_7 = 0.2$, $c_8 = 0.1$, $d_1 = 0.3$, $d_2 = 0.5$, $d_3 = 0.1$, $d_4 = 0.3, k_1 = 0.9, k_2 = 0.1, k_3 = 0.5, k_4 = 0.1, x(0) = 0.5, y(0) = 0.01$, $z(0)=0.05$ and $w(0)=0.5$. (a) The solution trajectory projected onto the (x,y)-plane. (b) The corresponding time courses of PTH (x), and (c) CT level (y).

V. CONCLUSION

In this paper, bone formation and resorption process is investigated mathematically. We have modified and analyzed a system of nonlinear differential equations accounting for the concentration of PTH above the basal level, the concentration of CT above the basal level, the number of active osteoclasts, and the number of active osteoblasts as in (1)-(4). Singular perturbation technique [24], [25] is then applied to our model to obtain the conditions on the system parameters for which the various kinds of dynamics behavior can be occurred including a periodic behavior in the solution of the system. Numerical simulations of the model are then carried out by using Runge-Kutta method which has been widely used to find the approximate solution of the differential equations [26]-[29]. The result shows that our model can deduce the nonlinear dynamic behavior which closely resembles to the pulsatile secretion patterns of PTH and CT observed in the clinical data [30], even though the model is kept relatively simple.

REFERENCES

[1] R. Marcus, *Osteoporosis*, Blackwell Scientific Publication, 1994.
[2] P. Morley, J.F. Whitfield and G.E. Willick, "Parathyroid hormone: an anabolic treatment for osteoporosis", *Curr Phar Design* , vol. 7, pp. 671-687, 2001.
[3] J.A. Albright and M. Sauders, *The Scientific Basis of Orthopaedics*, Norwalk, Conn.: Appleton & Lange, 1990.
[4] J.N.M. Heersche and S. Cherk, Metabolic Bone Disease: cellular and tissue mechanisms, Boca Raton, FI : CRC Press, 1989.
[5] A.M. Parfitt, "Targeted and nontargeted bone remodeling: relationship to basic multicellular unit origination and progression", Bone, vol. 30, pp. 5-7, 2002.
[6] L.K. Potter, L.D. Greller, C.R. Cho, M.E. Nuttall, G.B. Stroup, L.J. Suva and F.L. Tobin, "Response to continuous and pulsatile PTH dosing: A mathematical model for parathyroid hormone receptor kinetics", Bone, vol. 37, pp. 159-169, 2005.
[7] M.H. Kroll, "Parathyroid hormone temporal effects on bone formation and resorption", *Bull. Math. Bio*, vol. 62, pp.163-188, 2000.
[8] C. Rattanakul, Y. Lenbury, N. Krishnamara and D.J. Wollkind, "Mathematical modelling of bone formation and resorption mediated by parathyroid hormone: Responses to estrogen/PTH therapy", BioSystems, vol. 70, pp. 55-72, 2003.
[9] P. Pivonka, J. Zimak, D.W. Smith, B.S. Gardiner, C.R. Dunstan, N.A. Sims, T.J. Martin, G.R. Mundy, "Model structure and control of bone remodeling: A theoretical study", *Bone*, 43, 249-263, 2008.
[10] S.V. Komarova, "Mathematical model of paracrine interactions between osteoclasts and osteoblasts predicts anabolic action of parathyroid hormone on bone", *Endocrinology*, 146(8), pp. 3589-3595, 2005.
[11] E.M. Brown, "Extracellular Ca2+ sensing, regulation of parathyroid cell function, and role of Ca2+ and other ions as extracellular (first) messengers", *Physiol Rev*, vol. 71, pp. 371-411, 1991.
[12] H.M. Goodman, *Basic Medical Endocrinology*, 3rd edition, Academic Press, 2003.
[13] P.M. McSheehy and T.J. Chambers, "Osteoblastic cells mediate osteoclastic responsiveness to parathyroid hormone", *Endocrinology*, vol. 118, pp. 824-828, 1986.
[14] H. Yasuda, N. Shim and N. Nakagawa, "Osteoclast differentiation factor is a ligand for osteoprotogerin/osteoclast inhibitory factor and identical to TRANCE/RANKL", *Proc. Natl. Acad. Sci. USA*, 95(7), pp. 3597-3602, 1998.
[15] S.K. Lee and J.A. Lorenzo, "Parathyroid hormone stimulates TRANCE and inhibits osteoprotegerin massenger ribonucleic acid expression in murine bone marrow cultures: correlation with

osteoclast-like cell formation", *Endocrinology*, 140(8), pp. 3552-3561, 1999.

[16] D.W. Dempster, F. Cosman, M. Parisisen, V. Shen and R. Linsay, "Anabolic actions of parathyroid hormone on bone", *Endocr Rev*, vol. 14, pp. 690-709, 1993.

[17] N. Takahashi, N. Udagawa and T. Suda, "A new member of tumor necrosis factor ligand family, ODF/ OPGL/ TRANCE/ RANKL, regulates osteoclast differentiation and function", *Biochem Biophys Res Commun*, vol. 256, pp. 449–455, 1999.

[18] Y.Y. Kong, H. Yoshida, I. Sarosi, H.L. Tan, E. Timms, C. Capparelli, S. Morony, A. Santos, G. Van, A. Itie, W. Khoo, A. Wakeham, C. Dunstan, D. Lacey, T. Mak, W. Boyle and J. Penninger, "OPGL is a key regulator of osteoclastogenesis, lymphocyte evelopment and lymph-node organogenesis", *Nature*, vol. 397, pp. 315-323, 1999.

[19] T.L. Burgess, Y. Qian, S. Kaufman, B.D. Ring, G. Van, C. Capparelli, M. Kelly, H. Hsu, W.J. Boyle, C.R. Dunstan, S. Hu and D.L. Lacey, "The ligand for osteoprotegerin(OPGL) directly activates mature osteoclasts", *J Cell Biol* , vol. 145, pp. 527-538, 1999.

[20] G.D. Roodman, "Advances in bone biology: the osteoclast", *Endocr Rev*, vol. 17, no. 4, pp. 308-332, 1996.

[21] J.F. Whitfield, P. Morley and G.E. Willick, *The parathyroid hormone: an unexpected bone builder for treating osteoporosis*, Austin, Tex: Landes Bioscience Company, 1998.

[22] P. Morley, J.F. Whitfield and G.E. Willick, "Parathyroid hormone: an anabolic treatment for osteoporosis", *Curr Phar Design*, vol. 7, pp. 671-687, 2001.

[23] Y.T. Isogai, T. Akatsu, T. Ishizuya, A. Yamaguchi, M. Hori, N. Tokahashi and T. Suda, "Parathyroid hormone regulates osteoblast differentiation positively or negatively depending on differentiation stages", *J Bone Mineral Res*, vol. 11, pp. 1384-1393, 1996.

[24] T.J. Kaper, "An introduction to geometric methods and dynamical systems theory for singular perturbation problems. Analyzing multiscale phenomena using singular perturbation methods", *Proc. Symposia Appl Math*, vol. 56, 1999.

[25] S. Rinaldi and S. Muratori, "A separation condition for the existence of limit cycle in slow-fast systems", Appl Math Modelling, vol. 15, pp. 312-318, 1991.

[26] W. Sanprasert, U. Chundang and M. Podisuk, "Integration method and Runge-Kutta method", in *Proc. 15th American Conf. on Applied Mathematics*, WSEAS Press, Houston, USA, 2009, pp. 232.

[27] M. Racila and J.M. Crolet, "Sinupros: Mathematical model of human cortical bone", in *Proc. 10th WSEAS Inter. Conf. on Mathematics and Computers in Biology and Chemistry*, WSEAS Press, Prague, Czech Republic, 2009, pp. 53.

[28] N. Razali, R. R. Ahmed, M. Darus and A.S. Rambely, "Fifth-order mean Runge-Kutta methods applied to the Lorenz system", in *Proc. 13th WSEAS Inter. Conf. on Applied Mathematics*, WSEAS Press, Puerto De La Cruz, Tenerife, Spain, 2008, pp. 333.

[29] A. Chirita, R. H. Ene, R.B. Nicolescu and R.I. Carstea, "A numerical simulation of distributed-parameter systems", in *Proc. 9th WSEAS Inter. Conf. on Mathematic*al Methods and Computational Techniques in Electrical Engineering, WSEAS Press, Arcachon, 2007, pp. 70.

[30] K. N. Muse, S. C. Manolagas, L.J. Deftos, N. Alexander, and S.S.C. Yen, "Calcium-regulating hormones across the menstrual cycle", J. Clin. Endocrinol. Metab., vol.62, no.2, pp.1313-1315, 1986.